Field assessment of guar gum stabilized microscale zerovalent iron particles for in-situ remediation of 1,1,1-trichloroethane

Field assessment of guar gum stabilized microscale zerovalent iron particles for in-situ remediation of 1,1,1-trichloroethane

Published in

Journal of Contaminant Hydrology

164 (2014) 88-99

Milica Velimirovic[1,2], Tiziana Tosco[3], Maarten Uyttebroek[1], Michela Luna[3], Francesca Gastone[3], Cjestmir De Boer[4,5], Norbert Klaas[4], Hans Sapion[6], Heinrich Eisenmann[7], Per-Olof Larsson[8], Juergen Braun[4], Rajandrea Sethi[3], Leen Bastiaens[1,*]

1 VITO, Boeretang 200, 2400 Mol, Belgium

2University of Antwerp, Department of Bio-Engineering, Groenenborgerlaan 171, 2020 Antwerp, Belgium.

3Dipartimento di Ingegneria dell'Ambiente, del Territorio e delle Infrastrutture – Politecnico di Torino, corso Duca degli Abruzzi 24, 10129 Torino, Italy

4 VEGAS, University of Stuttgart, Pfaffenwaldring 61, 70569 Stuttgart, Germany

5 Department of Civil and Environmental Engineering, Western University, 1151 Richmond Street, London, ON, Canada N6A 5B9

6 SAPION, Oude Bevelsesteenweg 51, 2560 Nijlen, Belgium

7 ISODETECT, Ingolstaedter Landstrasse, 1, D85764 München, Germany

8 Höganäs AB, Bruksgatan 35, SE-263 83 Höganas, Sweden

[*] Corresponding author: Phone: +32 14 33 5634. E-mail: leen.bastiaens@vito.be.

E-mail addresses: Milica Velimirovic: milica.velimirovic@vito.be; Tiziana Tosco: tiziana.tosco@polito.it; Maarten Uyttebroek: maarten.uyttebroek@vito.be; Michela Luna: michela.luna@polito.it; Francesca Gastone: francesca.gastone@polito.it; Cjestmir De Boer: Cjestmir.deBoer@uwo.ca; Norbert Klaas: norbert.klaas@iws.uni-stuttgart.de; Hans Sapion: hans.sapion@sapion.be; Heinrich Eisenmann: eisenmann@isodetect.de; Per-Olof Larsson: Per-Olof.Larsson@hoganas.com; Juergen Braun: juergen.braun@iws.uni-stuttgart.de; Rajandrea Sethi: rajandrea.sethi@polito.it; Leen Bastiaens: leen.bastiaens@vito.be.

Abstract

A pilot injection test with guar gum stabilized microscale zerovalent iron (mZVI) particles was performed at test site V (Belgium) where different chlorinated aliphatic hydrocarbons (CAHs) were present as pollutants in the subsurface.100 kg of 56 µm-diameter mZVI (~70 g L^{-1}) was suspended in 1.5 m^3 of guar gum (~7 g L^{-1}) solution and injected into the test area. In order to deliver the guar gum stabilized mZVI slurry, one direct push bottom-up injection (Geoprobe) was performed with injections at 5 depth between 10.5-8.5 m bgs. The direct push technique was preferred above others (eg. injection at low flow rate via screened wells) because of the limited hydraulic conductivity of the aquifer, and to the large size of the mZVI particles. A final heterogeneous distribution of the mZVI in the porous medium was observed explicable by preferential flow paths created during the high pressure injection. The maximum observed delivery distance was 2.5 m. A significant decrease in 1,1,1-TCA concentrations was observed in close vicinity of spots where the highest concentration of mZVI was observed. Carbon stable isotope analysis (CSIA) yielded information on the success of the abiotic degradation of 1,1,1-TCA and indicated a heterogeneous spatio-temporal pattern of degradation. Finally, the obtained results show that mZVI slurries stabilized by guar gum can be prepared at pilot scale and directly injected into low permeable aquifers, indicatinga significant removal of 1,1,1-TCA.

Keywords:

guar gum, mZVI, 1,1,1-TCA, in-situ remediation, direct push, CSIA

Highlights:

- mZVI slurries stabilized with guar gum (GG) can be prepared at pilot scale.
- Highly concentrated GG-mZVI slurries can be injected via direct push technique.
- A heterogeneous distribution of the GG stabilized mZVI was observed.
- Abiotic degradation of 1,1,1-TCA was proven 1 m from injection at 4.5 m bgs.

1. Introduction

Permeable reactive barriers (PRBs) filled with granular zerovalent iron (ZVI) particles are currently used for the abiotic remediation of contaminated aquifers, and in particular for the treatment of dissolved chlorinated aliphatic hydrocarbons (CAHs) (Gillham and O'Hannesin, 1994). Typical applications are at shallow depths down to 10 to 15 m, exceptionally till 20 to 30 m below ground surface (bgs) (Day et al., 1999; Di Molfetta and Sethi, 2006;Zolla et al., 2009). In recent years, an increased interest emerged in using microscale and nanoscale ZVI particles (mZVI and nZVI, respectively) that can be injected into the subsurface, thus creating a reactive zone where harmful compounds are degraded to non-toxic ones. The advantages of such an approach, compared to PRBs, include (i) the absence of expensive construction techniques (i.e. the excavation of deep trenches for the emplacement of the reactive material), (ii) the possibility of the application underneath (operational) buildings, and (iii) the implementation at deeper levels. Generally, mZVI and nZVI particles are more reactive than granular ZVI (Hosseini and Tosco, 2013; Velimirovic et al., 2013). Therefore, they can be used for the interception of groundwater contamination plumes like PRBs, but might be more efficient when injected closer to the source area where higher pollutant concentrations are present. On the other hand, the technology may not be cost-efficient for treatment of source zones with significant amounts of DNAPLs (dense non-aqueous phase liquids) due to the chemical properties of DNAPLs and ZVIs. The presence of water is required for effective treatment of hydrophobic DNAPL phase after the injection of hydrophilic slurry of the mZVI and nZVI particles into the subsurface (Shemer and Semiat, 2013).

When implementing mZVI, a homogeneous and stable dispersion of the mZVI in the injection slurry is needed. Therefore, sedimentation of mZVI particles in the injection fluid during the injection should be prevented. To improve the stability of iron slurries and consequently the mobility in the subsurface after injection, dispersion of the iron particles in viscous non-Newtonian fluids is necessary (Gastone et al., 2014; Xue and Sethi, 2012). In particular, solutions of biopolymers, such as guar gum and xanthan

gum, have been found effective as stabilizing agents (Cantrell et al., 1997; Comba et al., 2011; Comba and Braun, 2012; Gastone et al., 2014; Kaplan et al., 1996; Luna, 2013; Saleh et al., 2007; Tiraferri and Sethi, 2008; Xue and Sethi, 2012). Guar gum and xanthan gum are shear thinning fluids and exhibit a higher viscosity at low shear rates (corresponding to low flow rates in the porous medium, or static conditions), which hinders particle sedimentation during preparation and storage of the dispersions. Conversely, the fluid viscosity decreases when increasing the shear rate (corresponding to high flow rates, and therefore to dynamic conditions during injection, both in pipes and in the subsurface), which limits the overall injection pressure (Gastone et al., 2014; Tosco et al., 2013).

Stabilized mZVI particles can be delivered into the subsurface by permeation or fracturing injection technologies (Christiansen et al., 2010; Suthersan, 1999). Permeation of the injection fluid is possible in highly permeable formations when sufficiently small particles (nanoscale or lower microscale) are injected at low pressure and a fairy homogenous distribution around the injection point might be expected (Tosco et al., 2014). Conversely, in scarcely permeable formations, where injection via permeation would require too low discharge rates, injection via fracturing is required. Further, fracturing is also necessary when the aquifer pore size is in the same order of magnitude as the size of the selected particles. For particle diameter to pore size ratio larger than 0.005-0.01, mZVI injection using a permeation approach would result in significant mZVI retention close to the injection well and consequently clogging of the porous medium, due to particles straining and mechanical filtration (Bradford et al., 2006; Xu et al., 2006). Injection via fracturing is realized by applying high injection pressures which induce preferential flow paths of the iron slurry, thus creating an inhomogeneous final distribution of the iron particles (Christiansen et al., 2010; Suthersan, 1999).

In the field study herein reported, the selected stabilizing agent was guar gum, a soluble polysaccharide extracted from the endosperm of a leguminose seeds (Chudzikowski, 1971). Guar gum has been proven to stabilize mZVI dispersions (Gastone et al., 2014; Tiraferri and Sethi, 2008; Velimirovic et al., 2012; Xue and Sethi, 2012), but its impact on mZVI reactivity was studied in detail more recently (Velimirovic et al., 2012, Velimirovic et al., 2014). Laboratory reactivity tests showed

that guar gum polymer chains adsorbed on the mZVI particles significantly hindered mZVI reactivity towards contaminants, though the process was proven to be completely reversible. Biodegradation of guar gum and intensive rinsing of the mZVI, simulating groundwater flow in the injection zone in the field, helped restoring the pristine reactivity, hereby removing the guar gum breakdown fragments from the particles. These laboratory findings suggest that also for field scale applications a temporarily decreased reactivity of the stabilized mZVI may occur.

Here we report a field test, where a highly concentrated guar gum stabilized mZVI slurry was injected in a contaminated site in Belgium. A fracturing injection approach was adopted, due to the limited hydraulic conductivity of the aquifer, and to the larger size of the mZVI particles selected for the application (d_{50}=56 µm). The study aimed at testing the possibility to inject highly concentrated iron slurries characterized by coarse particle size distribution in a low conductivity aquifer and at determining the distribution of mZVI particles in the subsurface after injection. Finally, the efficiency of mZVI in reducing contaminants such as 1,1,1-trichloroethane(1,1,1-TCA), 1,1-dichloroethane (1,1-DCA), trichloroethene (TCE), and *cis*-dichloroethene (cDCE) was examined. In order to distinguish between a reduction in concentration due to mixing with the injected fluid and a reduction due to degradation, compound-specific stable isotope (CSIA) measurements were conducted. Previously, the CSIA-measurements were proven to be a valuable tool to distinguish between dilution and degradation (Elsner et al. 2009;US EPA 2008), though its feasibility on spatial and temporal dynamics of degradation at a small-scale has not been demonstrated up to now.

2. Materials and Methods

2.1. Micro-iron particles and guar gum

The reactive mZVI particles (H20) used in the pilot scale study were obtained from Höganäs (Sweden). Characteristics of the particles are given in Table 1. Guar gum HV7000 (Rantec Corporation, USA) was used as mZVI stabilizer.

2.2. Test site description

The field site (further called "Site V") is an industrial site in Belgium not subject to regulation for drinking water protection areas. From 1975 to 1980 solvent-based wet painting coatings were produced in this plant, and since 1980 the production has been changed to powder coating.

Field investigation was conducted to characterize the site and the contaminant source (Supporting Information SI1 and SI2). The hydro-geological structure (SI3) of the site includes a shallow sandy aquifer (0 to 3 m bgs), a fine clayey-sandy aquitard (3 to 8 m bgs) and a deeper sandy aquifer (8 to 20 m bgs) with grain size distribution of d_{10} = 52 µm and d_{90} = 374 µm (SI4). The water table is approximately 2 m bgs.

The groundwater flow is preferentially towards south-southwest, with an estimated flow velocity of 10 m $year^{-1}$. The average hydraulic conductivity of 8.2 x 10^{-5} m s^{-1} was estimated by means of an aquifer pumping test and by slug tests (SI5). The hydraulic gradient ranges from 9 x 10^{-4} to 2.5 x 10^{-3}, while the effective porosity estimated on grain size distribution data is approximately 18 %.

The pollution consists mainly of CAHs originating from the painting production, in particular chlorinated ethanes (1,1,1-TCA) and chlorinated ethenes (TCE). The 1,1,1-TCA plume reaches the depth of 13.5 m bgs, while TCE plume reaches 15.5 m bgs. According to the monitoring campaign conducted one week before the injection of mZVI particles, the dominant pollutants are 1,1,1-TCA (> 20 mg L^{-1} in shallow layer) and its associated daughter product 1,1-DCA (> 10 mg L^{-1} in deep layers).

TCE (> 1 mg L^{-1}) and its associated daughter product cDCE (> 3 mg L^{-1} in deep layers) are present in lower concentrations. In the shallow layer, 1,1-DCE was also present at concentrations > 4 mg L^{-1}. According to the results of the characterization of the hydrodynamic properties of the aquifer and of the contaminant distribution, the layer of 8-10 m bgs was selected as the target for the pilot test injection.

2.3. Batch tests for biodegradation potential

Small scale batch reactivity experiments with aquifer material from the Site V were performed to assess whether the site microbial communityis able to degrade CAHs, and therefore to understand whether it can contribute to the overall degradation of the contaminants. Batch tests were prepared (triplicates) in a 160 mL glass vials capped with butyl/PFTE grey septum containing 30 g of soil and 70 g of groundwater collected at Site V (8-10 m bgs) before the injection was performed. The used groundwater was mainly polluted by 6.0 ± 0.4 mg L^{-1} of 1,1-DCA, 0.3 ± 0.1 mg L^{-1} of TCE, 1.8 ± 0.6 mg L^{-1} of cDCE, and 0.3 ± 0.0 mg L^{-1} of 1,1-dichloroethene (1,1-DCE). Beside a control without additional electron donor, two test conditions were set-up with sodium lactate (0.2 g kg^{-1}) and guar gum (2 g kg^{-1}), respectively, as a potential carbon source. Additionally, for each carbon source an abiotic control with formaldehyde (0.4 % v/v) was included. The batch reactors were incubated (shaking) at groundwater temperature (12°C). Analyses were performed at different time points: 0, 2, 4, 16, 34 and 47 weeks. Concentrations of 1,1-DCA, TCE, cDCE, 1,1-DCE, vinyl chloride (VC), acetylene, ethene, ethane, and methane were determined via headspace measurements as previously described by Velimirovic et al. (2013).

2.4. Sedimentation tests

The colloidal stability of iron slurries dispersed in guar gum solutions was tested by means of sedimentation tests. The mZVI dispersion in guar gum was prepared at different iron (50 and 120 g L^{-1})

and guar gum concentrations (2, 3, 4, 4.5 and 5 g L^{-1}). The guar gum solution was prepared by slowly adding the polymer powder to heated water (60°C), continuously stirring. The solution was prepared 24 h in advance, in order to guarantee the complete hydration of the powder overnight. After polymer hydration, iron particles were suspended into the guar gum solution using a high speed rotor-stator (UltraTurrax) to guarantee a good dispersion. The slurry was thenput in an elongated cuvette and the sedimentation process was continuously monitored at a fixed position using a magnetic susceptibility sensor (Dalla Vecchia et al., 2009).

2.5. Field-scale injection test

Before the field injection of mZVI particles, five multilevel detection systems (MLDS) comprising of groundwater sampling points, temperature sensors and detectors for the magnetic susceptibility (Buchau et al., 2010; Li et al., 2012) were installed within 2.5 m of radius around the planned injection point. More specifically, the position of the MLDS was 0.5, 1, 1.5, 2 and 2.5 m from the injection spot. Every MLDS consisted of 7 groundwater sampling ports at different depths (approximately 4.5, 8, 8.5, 9, 9.5, 10 and 10.5 m bgs) (Figure 1). MLDS5 had nogroundwater sampling port at 4.5 m bgs since it was damaged during the MLDS installation.

To emplace the guar gum stabilized mZVI into the ground, one-spot high pressure injection was performed using a direct push set-up (Geoprobe7822T and GS200 dual piston pump). A total volume of 1.5 m^3 solution containing guar gum (~7 g L^{-1}) and mZVI (~70 g L^{-1}) was injected divided over 5 different depths between 10.5 to 8.5 m bgs with 0.5 m vertical spacing (Table 2). As such, 0.3 $m^3$of guar gum stabilized mZVI was injected at each depth.

The day before the injection, the 1.5 m^3 of guar gum solution was prepared in small batches (50 L each) by dispersing 250 g of guar gum powder in 50 L of warm water (approximately 60 °C) and subsequently mixed with high shear rates (Collomix CX 200 hand-mixer – max. 580 rpm). Afterwards, the guar gum suspension was transferred to cube containers for transport to the field site and left 24 h

for complete hydration. In order to avoid sedimentation, mZVI was mixed with the guar gum suspension just before the injection in a funnel shaped stainless steel reservoir. For every injection level, approximately 20 kg of mZVI was mixed with 300 L of previously prepared guar gum solution and recirculated within the reservoir using a dosing pump (Seepex, Germany) and DK40 disperser (CAT, Germany) for 10 minutes before injection.

The injection was performed from bottom to top, applying an average flow rate of 8.6 L min^{-1}. The use of enzymes was found to be necessary to induce fast guar gum degradation after injection (Velimirovic et al., 2012). For this reason, a commercially available enzyme (LEB-H, Rantec) was directly dosed into the pump tank at the end of each injection. During each injection step, the pressure of the injected fluid was continuously monitored using a pressure transducer (Delta Ohm) connected to the injection pipe.

Finally, two weeks after injection, an extraction well was installed 20 cm from the injection point and 4 m^3 of groundwater were extracted to remove possibly remaining guar gum from the system, and simultaneously pull the contaminated groundwater into the mZVI-containing reactive zone.

After injection, the final iron distribution around the injection spot was investigated. Core samples were taken in two different campaigns (Figure 2), in order to identify the spatial distribution of iron via visual observation of the cores and hydrogen measurements after acid digestion of core sub-samples. Aliquots of 5 g of soil were taken from the cores at specific depths and dissolved with 5 g of 1 M HCl. After an incubation period of one month the produced amount of hydrogen (H_2) gas was quantified. By taking 500 µL headspace sample withdrawn from the 37 mL vials filled with 5 mL of samples, H_2 gas was analyzed using a gas Trace GC MPT-10286 (Interscience) equipped with HayeSepQ column (Alltech Associates, Inc.) and a thermal conductivity detector.

2.6. Groundwater sampling and analyses

To monitor the performance of the created mZVI reactive zone, groundwater samples were collected every five weeks by connecting the PTFE sampling tubing of the screened ports in the MLDS and conventional wells to a peristaltic pump. Field parameters were measured in a flow-through cell by a portable Multi 340i (WTW, Germany) equipped with a pH and temperature electrode SenTix41, a conductivity measuring cell TetraCon 325 and a Liq-Glass ORP electrode (Hamilton- Nevada, USA). Samples for CAHs analysis were collected in 30 mL vials (headspace free) capped with butyl/PFTE grey septa and stored at 12°C. Within 24 hours, 5 mL of collected sample was transferred to a 12 mL vial and analyzed forthe concentrations of CAHs (1,1,1-TCA, 1,1-DCA, TCE, cDCE, 1,1-DCE), intermediate products (VC, acetylene), and end-products (ethane and ethane) via direct head-space measurements using a Varian GC-FID. The concentration of guar gum present in the groundwater samples was quantified as described by Velimirovic et al., 2012. The geochemistry of the groundwater was characterized by quantifying chloride, sulfate, nitrate, nitrite, dissolved and total iron in groundwater samples.

Additionally, groundwater samples for compounds specific isotope analysis (CSIA) were collected from the MLDSs (at 3 depths: 4.5, 9, and 10.5 m bgs) directly into 37 mL vials and capped with a sealing cap. The groundwater extracted from the continuously screened wells (extraction well and control wells outside of the test area) was transferred in 1 L or 0.5 L glass bottles. Sodium hydroxide pellets were used for all samples preservation. Gas chromatography combustion isotope ratio mass spectrometry (GC-C-IRMS) was applied to determine the stable carbon isotope composition of CAHs. All samples were measured in duplicates. Isotope analysis was done via (i) accumulation by a purge-and-trap unit (Teledyne Tekmar); (ii) transfer to a gas chromatograph split injector at 100°C; (iii) injection at a split ratio of 1:7 to 1:100 to a capillary column (VOCOL 60 m x 0.25 mm ID or DB624 60 m Ø 0.25 mm ID Ø 1.4 µm FD); (iv) separation of compounds in GC by specific temperature shifts (TRACE GC Ultra, Thermo Fisher Scientific); (v) combustion of CAH to CO_2-molecules; (vi) transfer

and further separation of $^{12}CO_2$ vs. $^{13}CO_2$ in an isotope ratio mass spectrometer (Thermo Finnegan MAT 253).

Isotope ratios are reported as $\delta^{13}C$ values ‰ relative to the international standard V-PDB (Vienna Pee Dee Belemnite) according to:

$$\delta^{13}C = [(R_{sample} - R_{standard}) / R_{standard}] * 1000 \quad (1)$$

where R_{sample} and $R_{standard}$ are the $^{13}C/^{12}C$-ratios of the sample and an international standard, respectively.

Depending on the level of CAH-concentrations, variable injection split ratios and volumes were applied. Isotope values were retrieved by automatic and occasionally also manual peak integration. Authentic laboratory standards were used for identification of CAHs and to improve the accuracy of the isotope analyses by linear correction of isotope values.

The analytical uncertainty of isotope analyses in an identical sample given by the standard deviation (sd) of the replicate measurements generally is ≤0.5 ‰ (US EPA, 2008). However, field samples comprised additional variability arising from the sampling procedure. Isotope measurements regarded for interpretation had a mean standard deviation of ±0.46 ‰ (n = 341) with 37 values ranging in between ±1.0 ‰ and±3.0 ‰; values with higher sd were excluded.

2.7. Reactivity of used mZVI material

A batch degradation experiment was conducted to investigate the reactivity of mZVI after field injection. The mZVI containing soil sample was taken two weeks after injection and stored for 2 months at 12°C under anaerobic conditions prior to the test. The experiment was carried out in 160 mL vials, containing 5 g of aquifer material, 0.04 g of mZVI and 100 mL of polluted groundwater from the Site V (collected before injection). Vials filled with aquifer material without iron and polluted groundwater were used as a control. Headspace analyses were regularly performed (0, 7, 14, 35 and 70 days) as previously described (Velimirovic et al., 2013).

3. Results and discussion

3.1. Batch tests for biodegradation potential

The CAHs biodegradation potential at Site V was assessed via batch degradation experiments. After 47 weeks of incubation under in-situ conditions, the decreases in TCE, cDCE and 1,1-DCA concentration observed in reactors with only aquifer material (Figure 3) were limited and comparable with the abiotic control. Similar results were obtained from reactors which contained guar gum or lactate as extra electron donors (Figure 3). No production of vinyl chloride and methane (potential biodegradation products) was observed. Average mass recoveries of 87 % suggested a possible removal of TCE, cDCE and 1,1-DCA by sorption to the aquifer material, or losses during headspace samplings. This is concluded as the abiotic controls showed comparable recoveries. The low pH-value (pH = 4.92) of the groundwater might also be the reason of no active CAH-biodegradation in the aquifer material. Concentrations of chloride, sulfate, nitrate, nitrite, dissolved and total iron did not change after injection as compared to the pre-injection situation confirming no active CAH-biodegradation.

3.2. Sedimentation tests

Sedimentation tests were performed to identify the most effective guar gum concentration for high pressure injection of the mZVI slurry at Site V. The stability of the iron slurry was quantified by determining the sedimentation half time t_{50} (i.e. the time required for the iron concentration, C, to reach half of its initial value, C_0). For field applications, a sedimentation time higher than the expected injection time (1-1.5 hour) is required, in order to guarantee that mZVI particles are fairly homogeneously suspended in the slurry during all injection operations. Examples of the experimental sedimentation curves for several concentrations of guar gum and mZVI are reported in Figure 4, along with the corresponding sedimentation half times t_{50}. With increasing guar gum concentrations, the

sedimentation half time, and therefore the stability of the mZVI suspension, increases due to the increased viscosity of the iron slurry. Conversely, the influence of iron concentration is less pronounced.

Based on the sedimentation tests, a minimum guar gum concentration of 4.5 g L^{-1} was selected for the field injection, regardless the iron concentration. The results of a lab scale dose test (results not shown) indicated that a mZVI concentration of 70 g L^{-1} was suitable for degrading PCE, TCE, cDCE, 1,1-DCE, and 1,1,1-TCA, which is between the two concentrations (50 g $L^{-1}$and 120 g L^{-1}) that were considered for the sedimentation tests. In the field application, a safety factor of 1.6 was applied to the guar gum concentration determined in the laboratory, and the final value of approximately 7.2 g L^{-1} was selected.

3.3. Field injection: monitoring of injection pressure and final spatial distribution of mZVI particles

During the injection at each level, the injection pressure was continuously monitored. The pressure records for the depths 8.5-10 m are reported in Figure 5 and average flow rates are summarized in Table 2. The data of the first injection (10.5 m bgs) are omitted due to technical issues. At each depth, water was firstly injected followed by slurry injection and finally by further water flushing. The start and end of slurry injection can be clearly identified on the pressure graphs, corresponding, respectively, to a sharp pressure increase and decrease, due to the high viscosity of guar gum slurry compared to water. The generation of preferential flow paths in the subsurface usually corresponds to a peak in the pressure record, followed by a decrease down to an (almost) constant value, corresponding to fracture propagation in the subsoil (Daneshy, 2003; Fjar et al., 2008). The height of the peak and, thus the magnitude of the subsequent pressure decrease, depends as a general rule, on flow rate, viscosity and mechanical properties of the subsurface (Fjar et al., 2008, Ruiting, 2006; Suthersan, 1999).

Figure 5 a-c refer to pressure logs during injection in the deeper sand layer (depths 10, 9.5 and 9 m bgl, respectively). In each graph, after reaching the pressure peak(corresponding to fracture generation), the pressure slightly decreases. Conversely, for the injection performed in the bottom part of the clayey layer (8.5 m bgl, Figure 5 b andd), the peak pressure required for opening preferential flow paths was much higher (approximately 100 bar), due to the cohesive strength of the clay. The presence in all the graphs of different pressure peaks indicates multiple fracturing, while the higher pressure peak in the first part of the injection (second and fourth plots) indicates opening of a predominant fracture. The instantaneous pressure decrease about 30 minutes after injection 5 can be attributed to the fracture propagation in a less cohesive material, probably the fine sand, since the value reached is the same reached at the end of the previous injection. This hypothesis was later confirmed by core sampling analyses, which evidenced the presence of guar gum and iron at a shallow depth (4.5 m), above the clay layer. It is therefore possible to conclude that during the last injection (8.5 m bgs), the fracture first propagated in the clayey layer, and then moved upward toward the uppersandy layer, which evidenced less cohesive strength.

After the iron injection was completed, core samples were collected around the injection points, and the spatial (horizontal and vertical) distribution of mZVI was determined via acid digestion. The results, presented in Figure 6, indicate that mZVI reached a maximum radial distance from the injection well of 0.5 m (CS4, in the direction of MLDS4) at depths of 3.1 m (4 g of Fe per kg of aquifer material) and 4.5 m (8 g of Fe per kg of aquifer material).. The highest mZVI concentration was detected 0.5 m from the injection point (CS4) in the direction of MLDS4, at depths of 3.1 m (4 g of Fe per kg of aquifer) and 4.5 m (8 g of Fe per kg of aquifer). Visual observations of the cores confirmed these data (SI6). mZVI was also found next to the injection point (CS1) at 3.1 m depth. The presence of iron at depths 3-4 m bgs around the injection point indicates a clear non-homogenous distribution of mZVI around the injection spot. Preferential flow paths were clearly generated during injection, as suggested by the pressure data, and at least some of the fractures were oriented towards the upper layers of the aquifer system, where

the vertical load and formation resistance are lower and fracture propagation easier, as reported in Suthersan (1999).

The guar gum concentration was also measured in the water samples collected one day after the injection (Figure 7), and later, after the groundwater extraction from the newly installed pumping well (PW1). The samples were taken from the shallow ports of the monitoring multi-level wells (4.5 m bgs). The detection of guar gum in the water samples was used as an indirect indication of the direction and extent of the preferential flow paths during mZVI injection. In the first set of samples, the highest concentration of guar gum, equal to 608 mg L^{-1}, was detected in MLDS4 (1 m from the injection point, 4.5 m bgs). Lower concentrations were also found in MLDS3 and MLDS2 at 4.5 m bgs. This finding, along with the mZVI distribution results, proves that most of the slurry preferentially flowed upward towards the shallow layers of the aquifer system. In the second set of samples, collected after the groundwater extraction, the guar gum concentration in the sampling port of MLDS4 positioned at 4.5 m bgs dropped to 45 mg L^{-1}, while for all other samples the concentration was below the detection limit. Significant decrease of guar gum concentration was due to a combination of the guar gum removal by the enzymes activity, extraction step and groundwater flow.

3.4. Reactivity of injected mZVI

Field measurements of temperature, pH, redox potential (ORP) and electrical conductivity were conducted in each monitoring well as an additional indication of iron distribution (SI7). The results obtained during the monitoring phase before and after mZVI injection show that ORP and conductivity decreased significantly one day after injection in the MLDS4 (1 m from injection point) at depth 4.5 m bgs (Figure 8), where guar gum was also detected. Moreover, the electrical conductivity decreased significantly at the same point as an effect of lower conductivity of the delivered guar gum stabilized mZVI solution. A significant decrease of ORP within the ZVI delivery zone was also reported by Truex et al. (2011). A significant pH change was not observed after the injection, which is likely to be due to

the potential buffering capacity of the aquifer, coherently with previous column studies performed using the aquifer material from Site V (Velimirovic et al., 2014). However, pH data (5.4-6.5) suggested that a microbial reductive dechlorination in the subsurface was not likely to occur for most monitoring points, as the groundwater pH was far from the optimum pH range of 6.8-7.6 (Zhuang and Pavlostathis, 1995). A pH increase to 7.3-8.5 was observed for MLDS1 25 and 30 weeks after the injection (8-10.5 m bgs), as well as an increase to 6.8-7.1 for MLDS2 (10-10.5 m bgs) 5 weeks after the injection. This could be explained by guar gum removal from the mZVI delivery zone resulting in the reactivity recovery of mZVI particles and decrease in contaminants concentration.

The evolution of the total concentration of CAHs was followed in time for all monitoring wells (SI8). The injection of guar gum-stabilized mZVI slurry resulted in a significant reduction of the total CAHs in MLDS4 (1 m from injection point; 4.5 m bgs) (57%) and in MLDS5 (2.5 m from injection point; 8 m bgs) (62%). No significant decrease in CAHs concentration was observed at the other sampling ports and wells, indicating that preferential flow paths were created during the injection. Compared to pre-injection values, one day after the injection a significant decrease of 1,1,1-TCA was observed at MLDS4 (4.5 m bgs) (Figure 9). This may be caused by dilution, dislocation of contaminant to greater depths or degradation as a consequence of mZVI particles delivery. For other compounds, no significant decrease in concentration was observed excluding the dilution effect and confirms that initially guar gum negatively impacts mZVI reactivity as previously reported by Velimirovic et al. (2012).

To distinguish between degradation and dilution of CAHs in the test area, carbon stable isotope analyses were performed (US EPA, 2008). On the one hand, fourteen days after the injection, approximately 4 m^3 of groundwater were extracted 20 cm from the injection point to pull “fresh” contaminated groundwater into the reactive zone and avoid dilution of pollutants. CSIA analyses performed on the different fractions of the extracted groundwater revealed constant values ($\delta^{13}C$) for the pollutants, indicating that no major degradation processes were induced (Figure 10). However, there was one exception. 1,1,1-TCA exhibited a clear isotope enrichment ($\delta^{13}C$) in the first three samples (≤

1.3 m³) pointing towards degradation induced in the close vicinity of the injection well as a possible consequence of mZVI delivery (Figure 10). Similar observations were made for the measured pollutant concentrations. At the beginning of the extraction (≤ 1 m³), 1,1,1-TCA concentration exhibited 0.42mg L^{-1}. Later, 1,1,1-TCA concentration increased up to 14.6mg L^{-1}, whereas no change for other pollutants was observed.

On the other hand, samples extracted from the different wells and samplings points were also analyzed on carbon stable isotopes to evaluate the success of injected guar gum stabilized mZVI (SI9). Figure 11 shows mean CSIA results for the zone (4.5 m bgs) where the main part of the mZVI was actually situated. The $\delta^{13}C$ mean values measured after the extraction step are compared with pre-injection isotope measurements. No significant change in carbon isotope values was observed at 9 m bgs despite iron injection at that depth (SI9). However, iron distribution data show that particles were mainly delivered to more shallow depths where changes were noticed. $\delta^{13}C$ mean values indicate a clearly stimulated degradation of contaminants at 4.5 m bgs. Fast and remarkable enrichment of 1,1,1-TCA in close vicinity of the injection well (MLDS4) at 4.5 m bgs was observed (Figure 11). Isotopic evidence supports reaction of delivered mZVI with 1,1,1-TCA near this well. Degradation of pollutants at the same spot (MLDS4, 4.5 m bgs) is confirmed by isotope enrichment of further compounds (TCE: +3.0 ‰; cDCE: +4.1 ‰, 1,1-DCE: +6.2 ‰; 1,1-DCA: +6.2 ‰) compared to baseline values (SI9). $\delta^{13}C$ mean values at 1 m and 2.5 m from injection well at 10 m bgs indicate a possible degradation of 1,1,1-TCA at this depth as well. A consistent temporal development of other CAHs isotope values and concentrations (i.e. continuous increase of isotope signatures parallel to a continuous decrease of concentrations) at 9 m bgs and 10 m bgs was not found. The dynamics of hydrological conditions and performance of mZVI were too variable at these depths to be reflected as a continuous temporal development of investigated parameters in the present survey.

However, Elsner et al. (2010) demonstrated that isotope monitoring can trace enhanced, but spatially heterogeneous degradation of 1,1,1-TCA (and also TCE) at a field site after injection of ZVI. Since also the temporal progression of concentration and isotope values were variable in this study, most

hydrogeological settings of injection procedures apparently will deliver an irregular pattern of the spatio-temporal development of degradation (Elsner et al. 2010). On the other hand, the performance of permeable reactive barriers can be controlled more easily because of the simple passage of contaminants through a clearly defined reactive zone (VanStone et al. 2005).

3.5. Reactivity of used mZVI in the subsurface

The reactivity of mZVI present in the reactive zone (2 months after injection) was evaluated in batch degradation tests (Figure 12).

Degradation of TCE and cDCE was obtained in the soil samples with mZVI particles collected from CS4 (4.5 m bgs), while no degradation occurred in the control without mZVI. Increases in ethene and ethane as end products confirm that CAHs were degraded by the injected mZVI. Acetylene was also detected in the concentration of 25 mg L^{-1}highlighting that a β-elimination pathway was included.

4. Conclusion

The presented field test demonstrated that the use of guar gum stabilized mZVI slurries is realistic at a field scale. Firstly, it was shown that guar gum stabilized mZVI slurry can be relatively easily prepared at a pilot scale in the field, as the full scale preparation is predicted to be feasible. Next, the direct push technique allowed to injected iron slurries in the subsurface even in the presence of coarse iron particles (d_{50}= 56 µm) and low permeable formation. A controlled delivery of the product in the subsurface, on the other hand, is a challenge. Preferential flow paths of the injected iron slurry were created when applying high pressures of approximately 100 bars, maintaining an average flow rate of 8.6 L min^{-1} and injecting large volumes per interval (300 L). Consequently, a heterogeneous distribution of the iron particles was obtained and resulted in a heterogeneous spatio-temporal pattern of simulated 1,1,1-TCA degradation. While the deeper layer (8-10.5 m bgs) was targeted, a significant part of the mZVI migrated upward the shallow part of the aquifer (4.5 m bgs) due to preferential paths originated during injection. More specifically, the data point towards a preferential flow near MLDS4 located 1 m from the injection point. The maximum observed delivery distance of mZVI particles from the injection point is 2.5 m at 8 m bgs.

From CSIA data significant abiotic degradation of 1,1,1-TCA and other CAHs was proven to occur in the zone where the highest mZVI concentration was actually measured (4.5 m bgs). Faster reduction of 1,1,1-TCA by guar gum stabilized mZVI as compared to reduction of chlorinated ethenes (TCE, cDCE, 1,1-DCE) confirmed the results presented in previously reported batch (Velimirovic et al., 2012) and column (Velimirovic et al., 2014)studies.

Finally, batch tests data with mZVI collected from the injection zone, prove that guar gum stabilized mZVI is reactive 2 months after the injection.

In conclusion, despite the fact that guar gum stabilized mZVI particles were partly delivered at a different depth than intended, and therefore the mass of reactive particles delivered into the target area was lower than planned, the delivered mZVI was able to degrade 1,1,1-TCA at a field scale. This pilot

test indicates that guar gum stabilized mZVI particles may be considered as an alternative to nZVI particles for in-situ remediation of CAHs. Further demonstration of this technology in zones with different CAH-pollutants and with more controlled delivery approach of the reagents (injection equipment, targeted radius, injection pressure, suspension volume, etc.) is necessary and will be the objective of our future study.

Acknowledgments

This research was conducted in the framework of the European Union project AQUAREHAB (FP7 - Grant Agreement Nr. 226565). The support of Willy De Jongh at Site V was appreciated.

References

Bradford, S.A., Simunek, J., Bettahar, M., van Genuchten, M.T., Yates, S.R., 2006. Significance of straining in colloid deposition: Evidence and implications. Water Resour. Res. 42(12), art. n. W12S15, doi:10.1029/2005WR00479.

Buchau, A., de Boer, C.V., Klaas N., 2010. Inductive detection and concentration measurement of nano sized zero valent iron in the subsurface. IET Science, Measurement and Technology 4, 289-297.

Cantrell, K.J., Kaplan, D.I., Gilmore, T.J. 1997. Injection of colloidal Fe-0 particles in sand with shear-thinning fluids. J. Environ. Eng-Asce. 123, 786-791.

Christiansen, C.M., Damgaard, I., Broholm, M., Kessler, T., Klint, K.E., Nilsson, B., Bjerg, P.L., 2010. Comparison of Delivery Methods for Enhanced In Situ Remediation in Clay Till. Ground Water Monit. R. 30, 107-122.

Chudzikowski, R.J., 1971. Guar gum and its applications. Int. J. Cosmetic Sci.22, 43-60.

Comba, S., Braun, J., 2012. An empirical model to predict the distribution of iron micro-particles around an injection well in a sandy aquifer. J. Contam. Hydrol. 132, 1–11.

Comba, S., Dalmazzo, D., Santagata, E., Sethi, R., 2011. Rheological characterization of xanthan suspensions of nanoscale iron for injection in porous media. J. Hazard. Mater. 185 (2-3), 598-605.

Dalla Vecchia, E., Luna, M., Sethi, R., 2009. Transport in Porous Media of Highly Concentrated Iron Micro- and Nanoparticles in the Presence of Xanthan Gum. Environ. Sci. Technol. 43(23), 8942-8947.

Daneshy, A.A., 2003. Off-Balance Growth: A New Concept in Hydraulic Fracturing. J. Petrol. Technol. 55(4), 78-85.

Day, S.R., O'Hannesin, S.F., Marsden, L., 1999. Geotechnical techniques for the construction of reactive barriers. J. Hazard. Mater. 67, 285–297.

Di Molfetta, A., Sethi, R., 2006. Clamshell excavation of a permeable reactive barrier. Environ. Geol.50 (3), 361-369.

Elsner, M., LacrampeCouloume, G., Mancini, S., Burns, L., Sherwood Lollar, B. 2010., Carbon Isotope Analysis to Evaluate Nanoscale Fe(O) Treatment at a Chlorohydrocarbon Contaminated Site. Ground Water Monit. R. 30, 79-95.

Fjar, E., Holt, R. M., Raaen, A.M., Risnes, R., Horsrud P., 2008. Petroleum Related Rock Mechanics. 2nd ed., xxii, 491 p. pp., Elsevier, Amsterdam; Boston.

Gastone, F., Tosco, T., Sethi, R., 2014. Green Stabilization Of Microscale Iron Particles Using Guar Gum: Bulk Rheology, Sedimentation Rate And Enzymatic Degradation. J. Colloid. Interface. Sci. 421, 33-43.

Gillham, R.W., O'Hannesin, S.F., 1994. Enhanced degradation of halogenated aliphatics by zerovalent iron. Ground Water 32, 958–971.

Hosseini, S.M., Tosco, T., 2013. Transport and retention of high concentrated nano-Fe/Cu particles through highly flow-rated packed sand column. Water Res., 47 (1), 326-338.

Kaplan, D.I., Cantrell, K.J., Wietsma, T.W., Potter, A., 1996. Retention of Zero-Valent Iron Colloids by Sand Columns: Application to Chemical Barrier Formation.J. Environ. Qual. 25 (5), 1086-1094.

Li, H., de Boer, C.V., Buchau, A., Klaas N., Rucker, W.M., Hermes, H., 2012. Development of an inductive concentration measurement sensor of nano sized zero valent iron. 9th International Multi-Conference on Systems, Signals and Devices.

Luna, M. 2013. Injection of zerovalent iron particles: from laboratory scale to field application. PhD dissertation. Dipartimento di Ingegneria dell'Ambiente, del Territorio e delle Infrastrutture – DIATI. Politecnico di Torino.

Saleh, N., Sirk, K., Liu, Y., Phenrat, T., Dufour, B., Matyjaszewski, K., Tilton, R.D., Lowry, G.V., 2007. Surface modifications enhance nanoiron transport and NAPL targeting in saturated porous media. Environ. Eng. Sci. 24, 45-57.

Shemer, H.,Semiat, R., 2013. Destruction of organics in water via iron nanoparticles, in Duke, M., Zhao, D., Semiat, R. (Eds.), Functional Nanostructured Materials and Membranes for Water Treatment. Wiley-VCH, Weinheim, Germany.

Suthersan, S.S., 1999. Hydraulic and pneumatic fracturing. In: Remediation Engineering Design Concepts (Chapter 9). Lewis Publishers, USA.

Tiraferri, A., Sethi, R., 2009. Enhanced transport of zerovalent iron nanoparticles in saturated porous media by guar gum, J. Nanopart. Res. 11, 635-645.

Truex, M.J., Vermeul, V.R., Mendoza, D.P., Fritz, B.G., Mackley, R.D., Oostrom, M., Wietsma, T.W., Macbeth, T., 2011. Injection of Zero-Valent Iron into an Unconfined Aquifer Using Shear-Thinning Fluids. Ground Water Monit. R. 31 (1), 50-58.

Tosco, T., Petrangeli Papini, M., Cruz Viggi, C. Sethi, R., 2014.Nanoscale iron particles for groundwater remediation: a review. J. Clean. Prod. (in press)doi: 10.1016/j.jclepro.2013.12.026.

Tosco, T., Marchisio, D. L., Lince, F., Sethi R., 2013. Extension of the Darcy-Forchheimer Law for Shear-Thinning Fluids and Validation via Pore-Scale Flow Simulations. Transport Porous Med. 96(1), 1-20.

Truex, M.J., Vermeul, V.R., Mendoza, D.P., Fritz, B.G., Mackley, R.D., Oostrom, M., Wietsma, T.W., Macbeth, T., 2011. Injection of Zero-Valent Iron into an Unconfined Aquifer Using Shear-Thinning Fluids. Ground Water Monit. R. 31 (1), 50-58.

U.S. Environmental Protection Agency, 2008. A Guide for Assessing Biodegradation and Source Identification of Organic Ground Water Contaminants Using Compound Specific Isotope Analysis (CSIA). EPA/600/R-08/148.

VanStone, N., Przepiora, A., Vogan, J., Lacrampe-Couloume, G., Powers, B., Perez, E., Mabury, S., Lollar, B.S., 2005. Monitoring trichloroethene remediation at an iron permeable reactive barrier using stable carbon isotopic analysis. J. Contam. Hydrol.78, 313–325.

Velimirovic, M., Chen, H., Simons, Q., Bastiaens, L., 2012. Reactivity recovery of guar gum coupled mZVI by means of enzymatic breakdown and rinsing. J. Contam. Hydrol.142-143, 1-10.

Velimirovic, M., Larsson, P.-O., Simons, Q., Bastiaens, L., 2013. Reactivity screening of microscale zerovalent irons and iron sulfides towards different CAHs under standardized experimental conditions, J. Hazard. Mater. 252-253, 204-212.

Velimirovic, M., Simons, Q., Bastiaens, L., 2014. Guar gum coupled microscale ZVI for in-situ treatment of CAHs: continuous-flow column study. J. Hazard. Mater. 265, 20-29.

Xu, S.P., Gao, B., Saiers, E.J., 2006. Straining of colloidal particles in saturated porous media. Water Resour. Res. 42(12), doi: 10.1029/2006wr004948.

Xue, D., Sethi R., 2012. Viscoelastic gels of guar and xanthan gum mixtures provide long-term stabilization of iron micro- and nanoparticles. J Nanopart Res, 14(11), at. n. 1239, doi: 10.1007/s11051-012-1239-0

Zhuang, P., Pavlostathis., S.G., 1995. Effect of Temperature, pH and Electron Donor on the Reductive Dechlorination of Chloroalkenes. Chemosphere 31, 3537-3548.

Zolla, V., Freyria, F., Sethi, R., Di Molfetta, A., 2009. Hydrogeochemical and biological processes affecting the long-term performance of an iron based permeable reactive barrier. J. Environ. Qual. 38, 897-908.

Figures

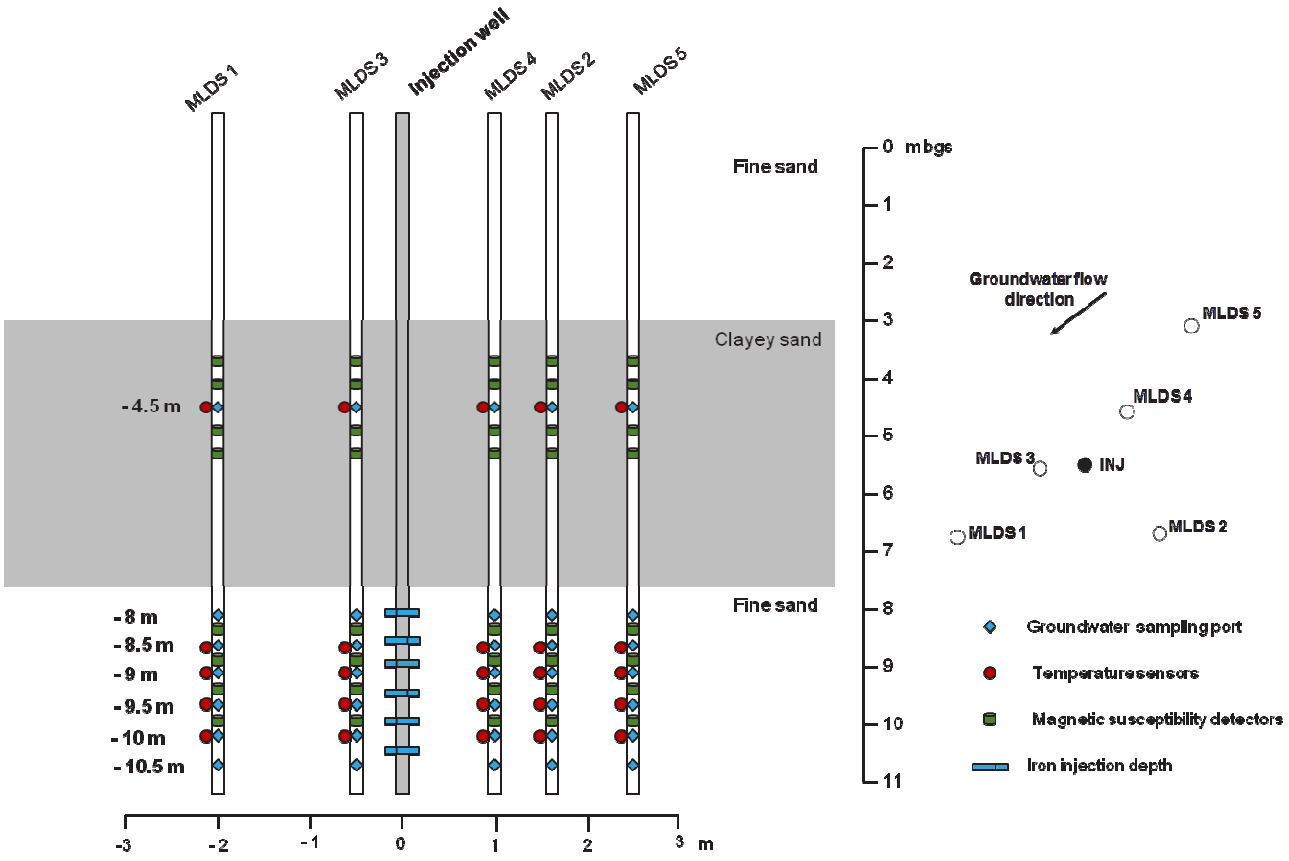

Figure 1. Monitoring wells location with indicated depth of groundwater sampling ports, temperature sensors and magnetic susceptibility detectors.

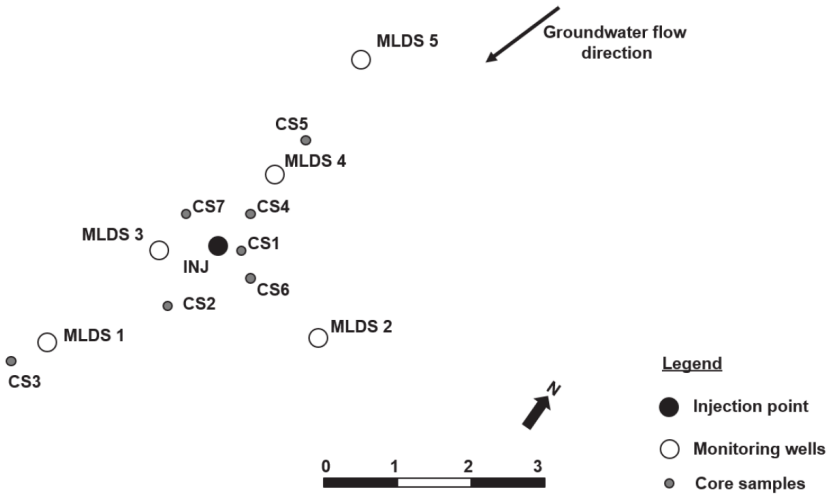

Figure 2. Location of soil cores extracted for evaluation of guar gum stabilized mZVI distribution: CS1 (0 – 11 m bgs); CS2-3 (4.5 – 11 m bgs) and CS4-7 (1 – 6 m bgs).

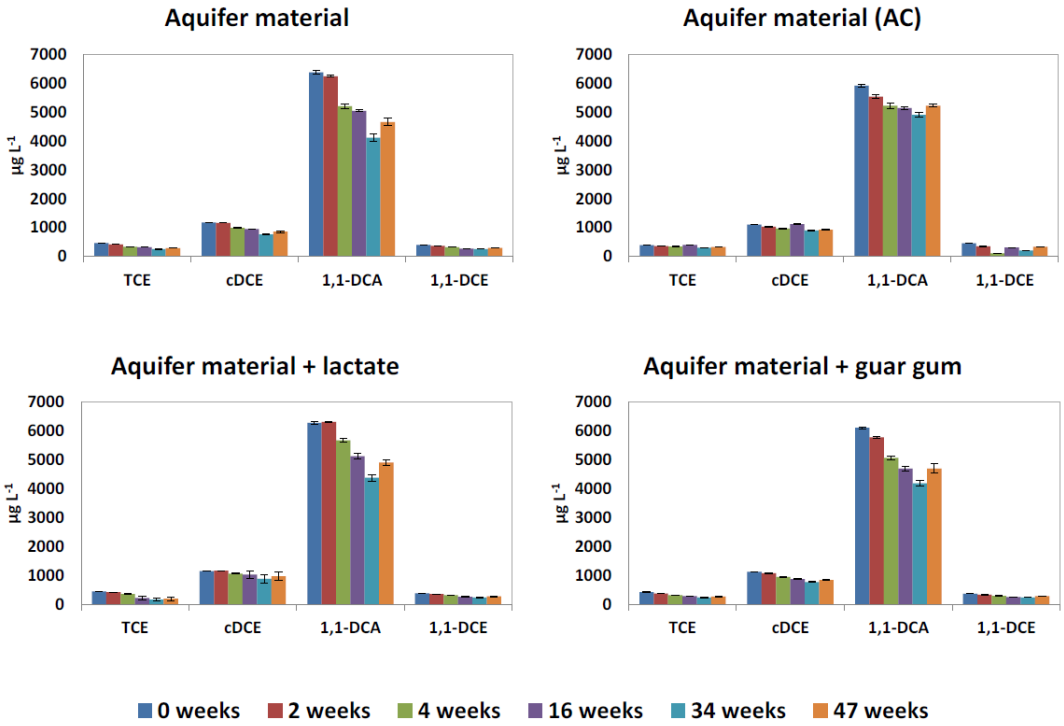

Figure 3. TCE, cDCE, 1,1-DCA and 1,1-DCE change over time in batches containing only aquifer material and supplemented with lactate or guar gum.

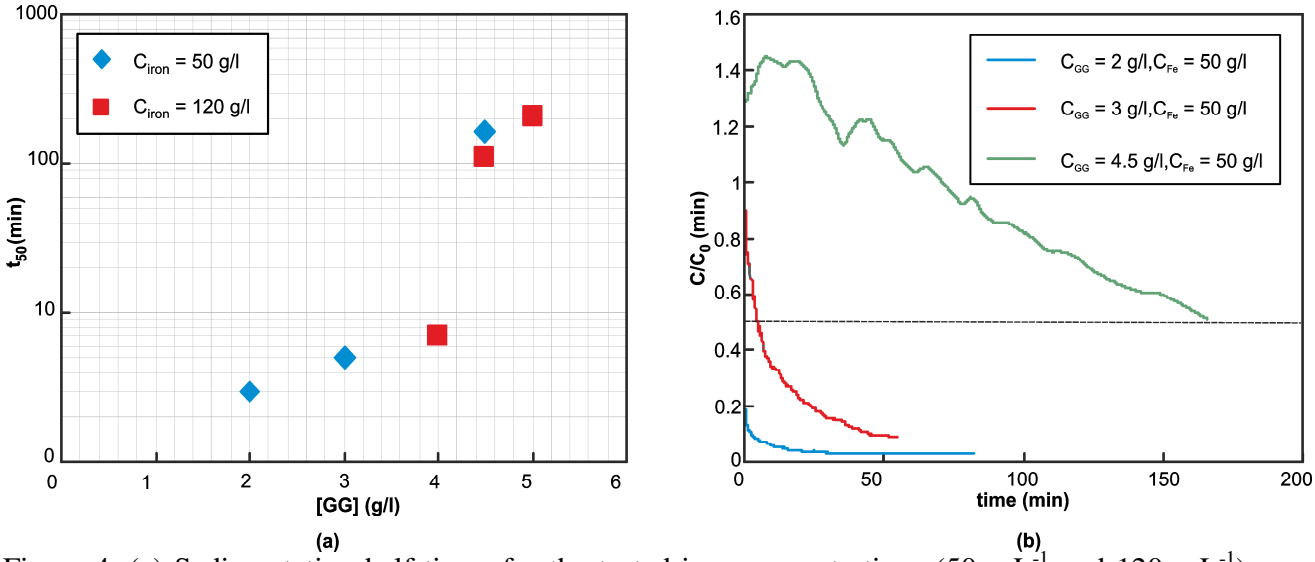

Figure 4. (a) Sedimentation half times for the tested iron concentrations (50 g L^{-1} and 120 g L^{-1}) as a function of guar gum concentration, and (b) example of sedimentation curves for mZVI (50 g L^{-1}) dispersed in guar gum solution at different guar concentrations (a). The dashed horizontal line represents the point where measured concentration is half the initial value.

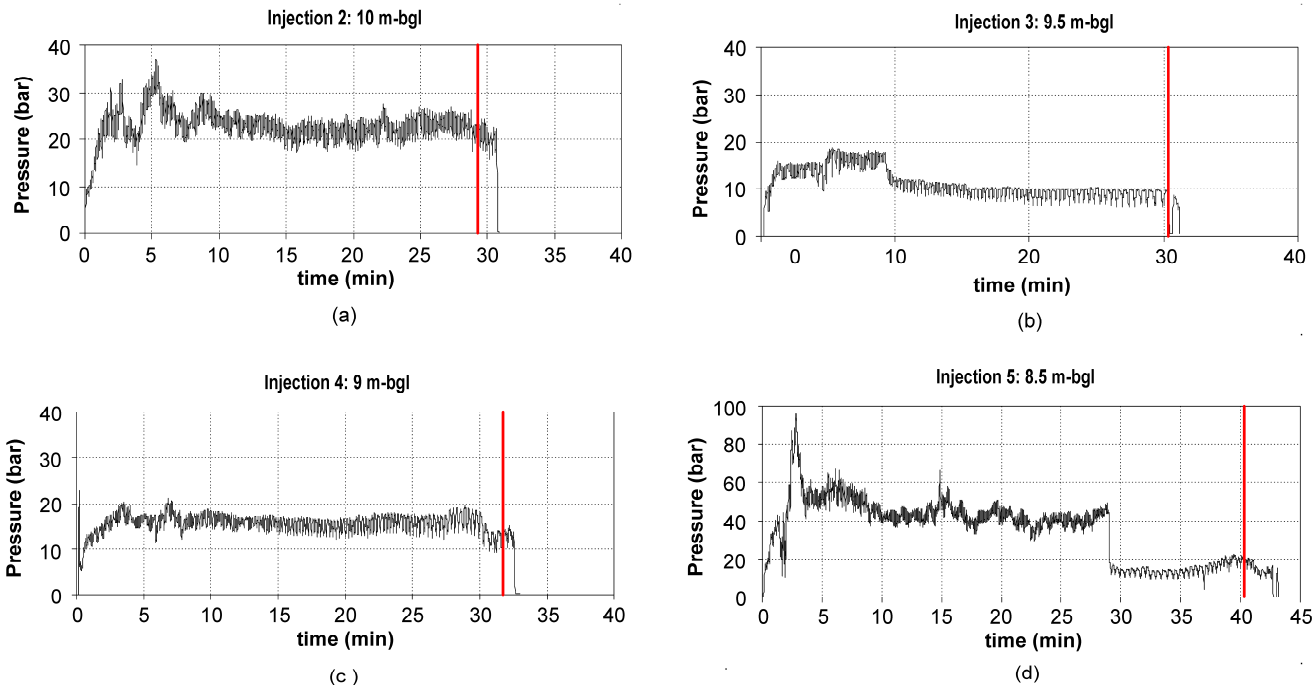

Figure 5. Pressure record during injection 2 (10 m bgs), injection 3 (9.5 m bgs), injection 4 (9 m bgs), and injection 5 (8.5 m bgs). The red line represent the end of the injection, from that time value started water injection.

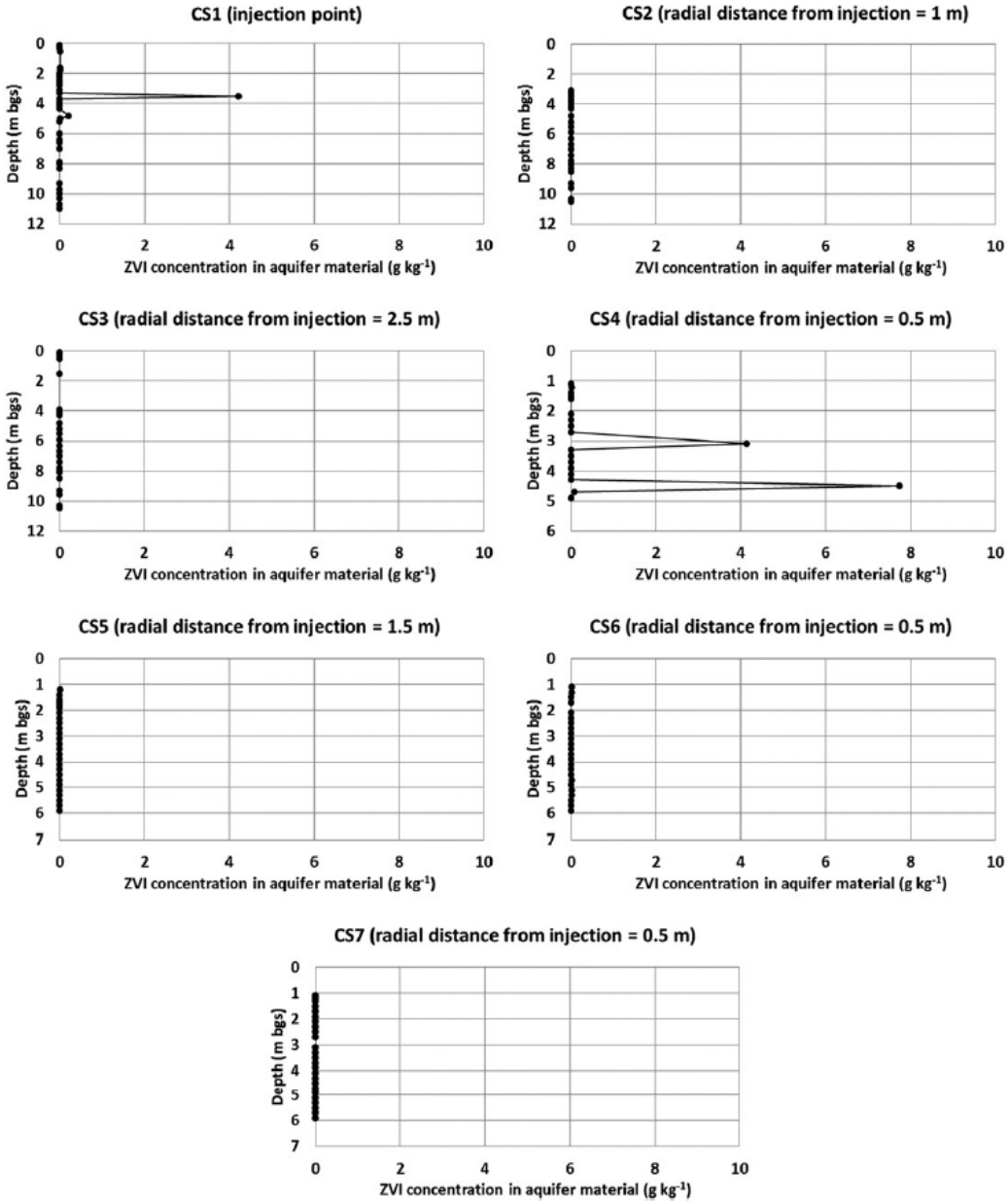

Figure 6. Distribution of mZVI in aquifer material determined via acid digestion from core samples extracted after mZVI injection.

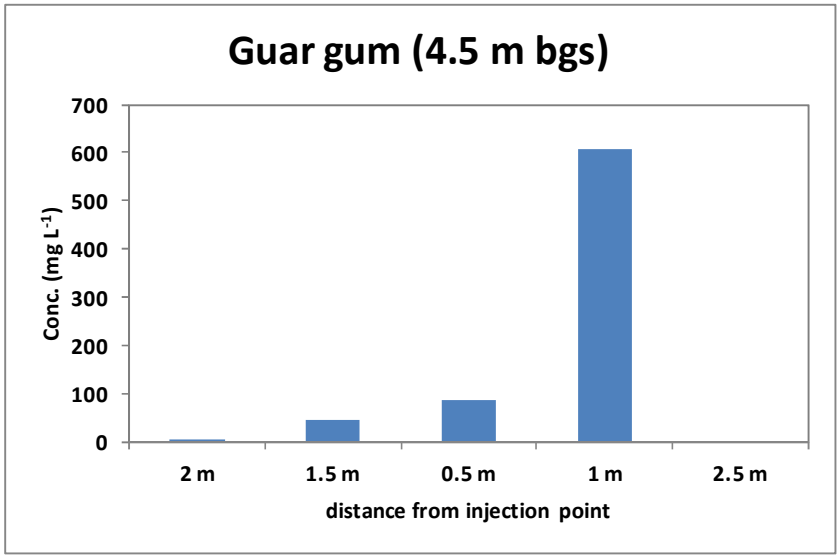

Figure 7. Guar gum detection in monitoring wells (MLDS1 – 2 m, MLDS2 – 1.5 m, MLDS3 – 0.5 m, MLDS4 – 1 m, and MLDS5 – 2.5 m from injection point) at 4.5 m bgs one day after iron injection.

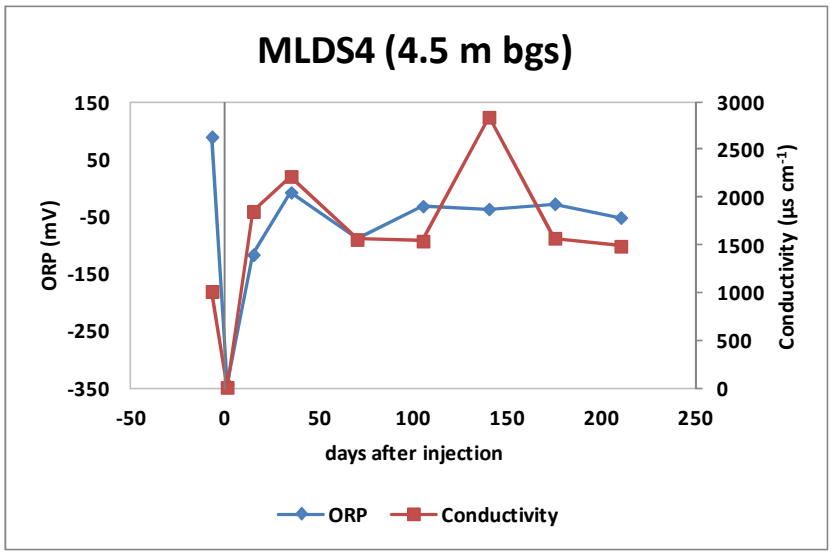

Figure 8. ORP and conductivity data over time for MLDS4 at 4.5 m bgs.

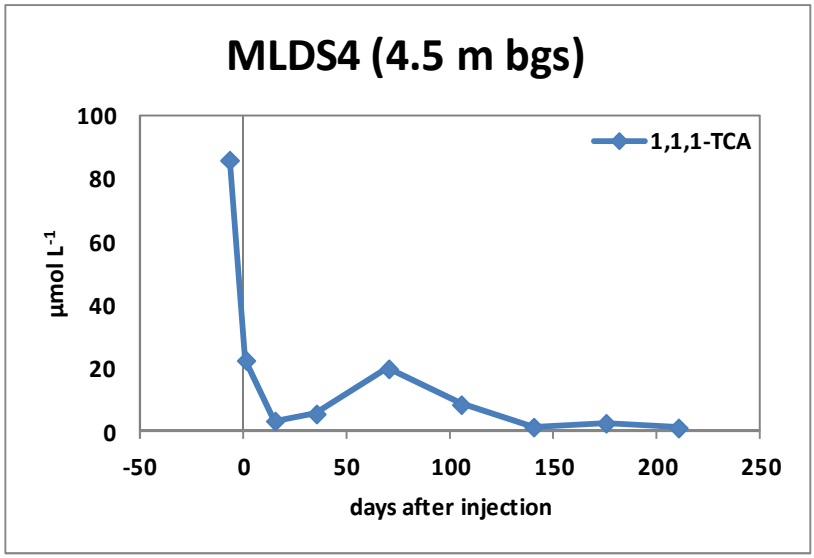

Figure 9. Changes in concentration of 1,1,1-TCA in groundwater over time in the MLDS4 at 4.5 m bgs.

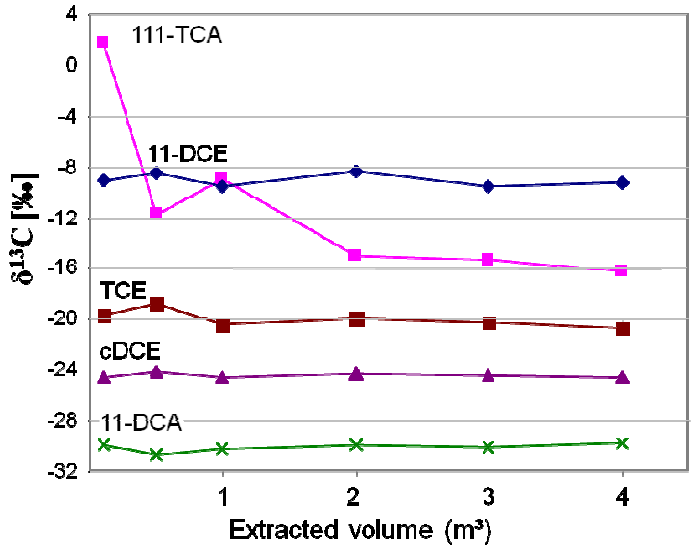

Figure 10. Carbon isotope values of five contaminants in extracted groundwater from an extraction well (20 cm from the injection point)14 days after guar gum stabilized mZVI injection.

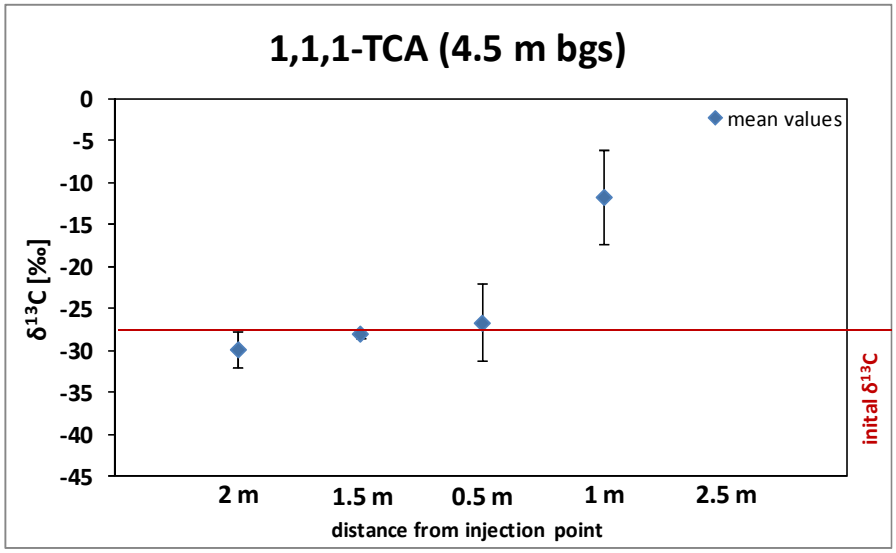

Figure 11. $\delta^{13}C$ (‰) mean values of 1,1,1-TCA in the monitoring wells (MLDS1 – 2 m, MLDS2 – 1.5 m, MLDS3 – 0.5 m, MLDS4 – 1 m, and MLDS5 – 2.5 m from injection point) at 4.5 m bgs. nm- not measured.

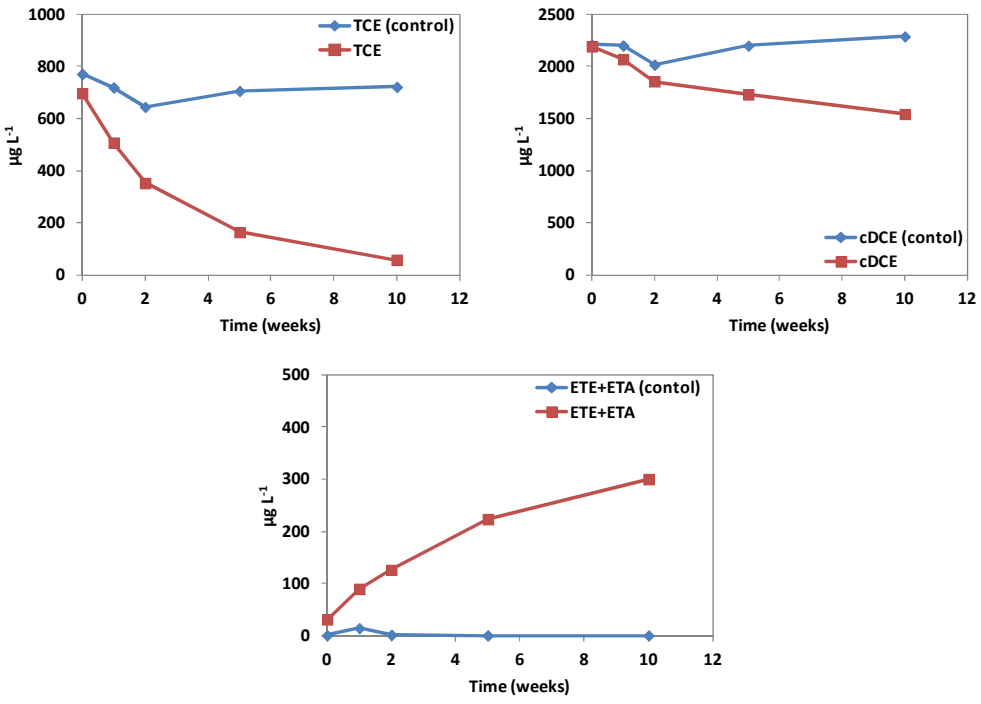

Figure 12. Reduction of TCE and cDCE in the presence of mZVI extracted from core samples after injection with production of ethene (ETE) and ethane (ETA) under laboratory conditions. Control conditions without mZVI are also presented.

Tables

Table 1. Characteristics of H20 iron (Höganäs, Sweden).

Sample	PSD[a] D_{10}, D_{50}, D_{90} (µm)	Carbon content (%)	Oxygen content (%)	Sulfur content (%)	Nitrogen content (%)	BET[b] (m^2 kg^{-1})
H20	24, 56, 69	0.02	1.10	0.00	0.02	57

[a]Particle Size Distribution.
[b]BET : Specific Surface Area according to Brunauer-Emmett-Teller (Single point measurement) - analysis was conducted by Höganäs.

Table 2. Bottom-up injection at the Site V. Overview of the injection depths, amount of iron injected and average discharge rate of the guar gum stabilized mZVI slurry.

Injection #	Depth (m bgs)	Amount of mZVI (kg)	Average discharge rate (L min-1)
1	10.5	19.6	8.69
2	10.0	22.0	9.63
3	9.5	20.6	8.93
4	9.0	21.2	8.40
5	8.5	21.2	7.45